

1 Integrative methylome and transcriptome analysis of

2 Japanese flounder (*Paralichthys olivaceus*) skeletal

3 muscle during development


4

5 Jingru Zhang, Shuxian Wu⁶, Yajuan Huang⁶, Haishen Wen⁶, Meizhao Zhang⁶, Jifang Li⁶, Yun

6 Li⁶, Xin Qi⁶, Feng He*

7 Ministry of Education Key Laboratory of Mariculture, College of Fisheries College, Ocean University

8 of China, Qingdao, Shandong, China,

9  These authors contributed equally to this work.

10 * Feng He@ouc.edu

11 Abstract

12 **DNA methylation is an important epigenetic modification in vertebrate and**

13 **is essential for epigenetic gene regulation in skeletal muscle development. We**

14 **showed the genome-wide DNA methylation profile in skeletal muscle tissue of**

15 **larval 7dph (JP1), juvenile 90dph (JP2), adult female 24 months (JP3) and adult**

16 **male 24 months (JP4) Japanese flounder. The distribution and levels of**

17 **methylated DNA within genomic features (1st exons, gene body, introns, TSS200,**

18 **TSS1500 and intergenic) show different developmental landscapes. We also**

19 successfully identified differentially methylated regions (DMRs) and different
20 methylated genes (DMGs) through a comparative analysis, indicating that DMR
21 in gene body, intron and intergenic regions were more compared to other regions
22 of all DNA elements. A gene ontology analysis indicated that the DMGs were
23 mainly related to regulation of skeletal muscle fiber development process, Axon
24 guidance, Adherens junction, and some ATPase activity. Methylome and
25 transcriptome clearly revealed a exhibit a negative correlation. And integration
26 analysis revealed a total of 425, 398 and 429 negatively correlated genes with
27 methylation in the JP2_VS_JP1, JP3_VS_JP1 and JP4_VS_JP1 comparison
28 groups, respectively. And these genes were functionally associated with pathways
29 including Adherens junction, Axon guidance, Focal adhesion, cell junctions,
30 Actin cytoskeleton and Wnt signaling pathways. In addition, we validated the
31 MethylRAD results by bisulfite sequencing PCR (BSP) in some of the
32 differentially methylated skeletal muscle growth-related genes (Myod1, Six1 and
33 Ctnnb1). In this study, we have generated the genome-wide profile of methylome
34 and transcriptome in Japanese flounder for the first time, and our results bring
35 new insights into the epigenetic regulation of developmental processes in
36 Japanese flounder. This study contributes to the knowledge on epigenetics in
37 vertebrates.

38 Author summary

39 Epigenetic mechanisms like DNA methylation have recently reported as vital
40 regulators of some species skeletal muscle development through the control of genes

41related to growth. To date, although genome-wide DNA methylation profiles of many
42organisms have been reported and the Japanese flounder reference genome and whole
43transcriptome data are publically available, the methylation pattern of Japanese
44flounder skeletal muscle tissue remains minimally studied and the global DNA
45methylation data are yet to be known. Here we investigated the genome-wide DNA
46methylation patterns in Japanese flounder, throughout its development. These findings
47help to enrich research in molecular and developmental biology in vertebrates.

48Introduction

49 As to genetic regulations, a growing number of studies have reported
50that epigenetic modifications play critical roles in gene expression. Epigenetics refers
51to heritable changes that modify DNA or associated proteins but without changing the
52fundamental DNA sequence itself [1]. The epigenome is a dynamic entity influenced
53by predetermined genetic programs and external environmental cues [2]. DNA
54methylation is an important epigenetic modification of the genome found in most
55eukaryotes and plays a key role in muscle development. It occurs at the C5 position of
56cytosine within CpG and non-CpG in the genome. The regulation and mechanisms of
57the DNA methylation still remain enigmatic, although it is essential for normal
58development and crucial in many biological processes, such as gene expression
59regulation, embryogenesis, cellular differentiation, genomic imprinting, X-
60chromosome inactivation, maintenance of genomic stability by transposon silencing
61[3-6]. Now, DNA methylation has attracted much attention owing to its broad impact,
62reversibility, heritability and genetic characteristics.

63 The profile of DNA methylation across the genome is important to understand
64DNA methylation dynamics during different developmental muscle development. The
65genome-wide DNA methylation profiles and functional analysis of many organisms,
66such as human [7], rat [8], Arabidopsis [9] has been reported. However, little is
67known about the DNA methylation patterns in Japanese flounder.

68 Japanese flounder is one of the commercially important marine fish in
69China and has been widely cultured in recent years. Skeletal muscle represents the
70most abundant tissue in the body and its features have a direct impact on meat quality.
71Understanding the growth and development of skeletal muscle is important. Skeletal
72muscle development is a very complicated but precisely regulated process, which
73contains four steps: determination of myoblasts, proliferation of myoblasts,
74differentiation and fusion of myoblasts into myotubes and myofibers, and growth and
75maturation until postnatal [10–11]. The research of complex mechanism underlying
76skeletal muscle development is helpful to genetic improvement for meat quality. In
77Japanese flounder, the muscle mass and meat quality are mostly determined by the
78size and the number of myofibers. Hence, we chose three postnatal stages (larval,
79juvenile and adult stage) which are key points in Japanese flounder skeletal muscle
80growth and development. The comprehensive analyses of these specific stages should
81help to understand the developmental characteristics in Japanese flounder skeletal
82muscle.

83 Many previous studies have concentrated on the impacts of DNA methylation
84and even located sites in the promoter or the first exon of a gene. It generally leads to

85transcriptional silencing and suppresses the corresponding protein products in most
86eukaryotes [6,12-14]. Thus, DNA methylation plays critical roles in cellular processes
87and the development of skeletal muscle tissue.

88 There are many approaches to decipher a genome-wide DNA methylation
89profile, including Methylation-dependent restriction-site associated DNA sequencing
90(MethyRAD), MeDIP-seq and whole-genome bisulfite sequencing (WGBS). The
91gold standard to determine the DNA methylome is genome-wide bisulfite sequencing,
92which firstly converts all the unmethylated cytosines into uracil while left the
93methylated cytosines unchanged by sodium bisulfite under denaturing conditions,
94which can be distinguished subsequently by sequencing[15]. [whereas](#) genome-wide
95bisulfite sequencing is highly expensive and time-consuming. Now,
96studies have shown that MethyRAD is a suitable method for high-throughput
97sequencing to analyze the DNA methylation status of methylated genome regions
98at a fraction of the cost and time of genome-wide bisulfite sequencing. MethyRAD
99uses methylation-dependent restriction enzymes which can specifically discriminate
100methylated cytosines between CG and non-CG methylation. These enzymes have the
101unique ability to produce 32-base-long fragments around fully methylated restriction
102sites, which are suitable for high-throughput sequencing to profile cytosine
103methylation on a genomic scale [16,17]. Many recent studies have shown that
104MethyRAD can reflect the relative genome-wide DNA methylation profile [18,19].
105Therefore, we chose MethyRAD to analyze genome-wide profiles of DNA
106methylation in Japanese flounder in our study.

107 In this study, we have performed the first integrated genome-wide analysis of
108 DNA methylation, and mRNA transcriptional activity, using the transcriptome and
109 MethylRAD (a simple genomic methylation site detection method) [16,20] data by
110 high-throughput, deep-sequencing technologies and subsequent bioinformatics
111 analysis. A series of genes involved in the development of skeletal muscle were
112 confirmed to show simultaneously differential expression levels and DNA
113 methylation levels. These findings provided comprehensive insights into the skeletal
114 muscle development during different developmental stages. Skeletal muscle tissues
115 were used in this study, namely, the larval 7dph (JP1), juvenile about 90dph (JP2),
116 adult female about 24 months (JP3) and adult male about 24 months (JP4).

117 **Results**

118 **Global mapping of DNA methylation in Japanese flounder**

119 The MethylRAD analysis was used to study the global mapping of DNA
120 methylation pattern in the Japanese flounder skeletal muscle tissues of JP1, JP2, JP3
121 and JP4. We generated about 439 - 751 million raw reads from each samples. After
122 low-quality data filtration, about 42 to 54 million reads assessed as clean data were
123 analyzed and mapped (S1 Table). Base distribution and quality distribution maps of
124 clean reads were plotted (S1 Fig). Of the high-quality methylation tag libraries in the
125 twelve samples, 71.76-81.08% were comparable to unique positions with a high-
126 quality read alignment against the Japanese flounder reference genome using SOAP
127 software (version 2.21) (S1 Table).

128 The percentage of the DNA methylation sites (CCGG sites and CCWGG sites) in

129each sample are shown (S2 Fig). We found a substantial amount of CCGG methylation
130and a small amount of CCWGG methylation. Therefore, we analyzed the genome
131coverage of the CCGG, CCWGG sites under different sequencing depth (S2 Table).
132The sequencing depths of the DNA methylation sites (CCGG sites and CCWGG sites)
133in each sample are shown in a box plot (the number of methylation sites in each
134sample had a depth higher than 3) (Fig 1). The JP1, JP2, JP3 and JP4 methylation
135sites (CCGG/CCWGG) were identified on the chromosomes of Japanese flounder.
136Methyl-RAD reads were detected in most chromosomal regions (chromosomes 1–24)
137in each group (Figure 2).

138**Distribution of DNA methylation sites of different functional regions**

139 The distribution of MethyIRAD reads that were aligned on a unique locus in
140different genome regions represents a genome-wide methylation pattern. We obtained
141the DNA methylation site annotation of the Japanese flounder genome and the
142comparison of average methylation sites showed that there were differential
143methylation site distribution in different components of the genome. The distribution
144patterns of most methylated sites at the different elements of genomes were similar in
145the four groups. We found that the major proportion of DNA methylation sites were
146mainly enriched in the intergenic regions followed by the regions at the gene body,
147TSS1500 (upstream 1500 bp of transcription start sites TSS), intron, 1stexon and
148TSS200 (upstream 200 bp of TSS) at both the CCGG and CCWGG sites (Fig3A).
149Among all the classes, the average methylation sites of promoter was the lowest.
150Furthermore, all gene regions in the JP1, JP3 and JP4 group exhibited higher number

151of methylation site than those in the JP2 group, while JP3 group showed lower
152number of methylation site than those in the JP4 group (Fig 3B). The distribution of
153methylation sites on different gene elements in each sample indicates that the skeletal
154muscle growth difference during different developmental stages might be associated
155with global methylation.

156**Relative quantification of DNA methylation levels around the Gene body**

157 We found that the DNA methylation site distribution curve had TSS representing
158an upstream sequence centered on the transcription initiation site, and TTS
159representing a downstream sequence centered on the transcription termination site.
160Hence, we analyzed the distribution of DNA methylation in the 2 kb region upstream
161of the TSS, gene body (the entire gene from the TSS to the transcription termination
162site (TTS). The region around the TSS is crucial for gene expression regulation. The
163DNA methylation level dramatically decreased in the 2 kb region upstream of the
164transcription start sites (TSS) and dropped to the lowest point before the TSS and
165increased sharply towards the gene body regions and stayed at a plateau until the TTS.
166The DNA methylation levels at either the CCGG sites or the CCWGG sites in the
167gene regions were similar for four groups (Fig 4).

168**Differentially methylated regions (DMRs) analysis**

169 To characterize the differences of DNA methylation levels among samples,
170DMRs were detected. For assessing the methylation level of differential methylation
171sites between four groups for the three biological replicates, the cluster heat map was
172shown to further show the changes in CCGG/CCWGG methylation levels among the

173groups. Hypomethylated CCGG/ CCWGG sites in samples are clustered at the
174bottom, whereas hypermethylated CCGG/CCWGG in samples are massed on upper
175cluster heat map. Interestingly, hierarchical cluster analysis results indicated that there
176were unique methylation patterns among four groups, and showed distinctive
177interindividual and intraindividual differences in methylation profiles among groups
178(S3 Fig).

179 The number of hypermethylation DMRs is less than hypomethylation DMRs.
180The number of DMRs in CCGG sites is lower than that in CCWGG sites. DMRs that
181are unique or shared among the four groups are shown (Fig 5). The results of a box-
182plot analysis of DMRs showed that the methylation level of the JP2 group was the
183lowest among four groups and the JP3 group is lower than that in JP4 group (S4 Fig).
184The pie map distribution of differential methylation sites with differential methylation
185levels on different functional components was drawn according to the positional
186information of the differentially methylated site-related gene, and the results are
187shown (S5 Fig). The results showed that the CCGG/CCWGG site were mostly
188enriched in the intergenic regions, followed by the gene coding regions (1stExon +
189other exons), the TSS1500 (upstream 1500 bp of TSS), intron and TSS200
190(upstream 200 bp of TSS) (S5 Fig).

191**Analysis of differential methylation site-related genes**

192 To investigate the differential methylation site-related genes regulatory role, the
193function of a gene was described by the GO and KEGG enrichment analysis of the
194gene where the differential DNA methylation sites were located. We found that these

195methylation site-related genes were significantly enriched in some biological
196processes and signaling pathway important for skeletal muscle development. The GO
197enrichment analysis top30 bar graph is shown (S6 Fig). The “Focal adhesion”, “actin
198cytoskeleton”, “Adherens junction”, “**cell junctions**”, “**Wnt signaling pathways**”,
199“Axon guidance”, “Wnt signaling pathway” and “Hippo signaling pathway” were
200significantly enriched in Japanese flounder (S7 Fig).

201**MethylRAD-seq data validation by bisulfite sequencing**

202 To validate the results obtained with MethylRAD-seq data, according to the GO
203and KEGG enrichment analysis of the DMGs, three genes (Myod1, Six1 and Ctnnb1)
204related to skeletal muscle developmet were selected from MethylRAD-Seq data in the
205Japanese flounder genome for analysis by bisulfite sequencing. Ctnnb1 was up-
206methylated in the JP2_VS_JP1, JP3_VS_JP1 and JP4_VS_JP1 comparison groups,
207respectively; Six1 was up-methylated in the JP3_VS_JP1 and JP4_VS_JP1
208comparison groups, respectively; and MyoD1 was up-methylated in the JP4_VS_JP3
209comparison group and as down-methylated in the JP3_VS_JP2 comparison group.
210The bisulfite sequencing results showed a high degree of consistency with the
211MethylRAD data (Fig 6). These results indicated that our genome-wide methylation
212results obtained by MethylRAD are reliable.

213**Transcriptome assembly and annotation**

214 Using RNA-Seq, this study compared the transcriptomic landscapes of skeletal
215muscle from the larval、 juvenile and adult (female and male) stages used to
216construct mRNA libraries. All the samples sequenced on the Illumina HiSeq X Ten

217platform and 150 bp paired-end reads were generated. The sequencing reads were
218analyzed using Tophat software by alignment with the Japanese flounder reference
219genome. Raw reads were processed using the NGS QC Toolkit to reduce the impact of
220sequencing errors. After filtering low quality reads, reads containing adapter, reads
221containing ploy-N, among the aligned reads, a total of 91,134,425 (JP1), 91,104,445
222(JP2), 91,857,072 (JP3) and 92,720,615(JP4) average clean reads were mapped, and
223on average approximately 77.63%(JP1), 71.42%(JP2), 78.50% (JP3) and 76.18%
224(JP4) of the reads individually were totally mapped to the Japanese flounder genome
225and approximately 74.67%(JP1), 65.34%(JP2), 65.80%(JP3) and 66.10%(JP4) of the
226reads in each sample were uniquely mapped to the Japanese flounder genome in each
227sample. Multiply mapped(JP1:2.96%, JP2:6.09%, JP3:12.69%, JP4:10.08%) reads
228were excluded from further analyses and other Parameters are presented (S3 Table).

229Comparative and enrichment analysis of differentially expressed genes.

230 We defined genes with fold changes > 2 and P-values < 0.05 were recognized as
231significantly differentially expressed. Different expression genes that are unique or
232shared among the four groups examined are shown(Fig7).

233 The DEGs among groups were conserved and were mainly enriched in the
234cellular component, molecular function, and biological process categories (S8 Fig).
235And the analysis of KEGG pathway revealed that multiple pathways involved in
236growth and development were clearly enriched in the Japanese flounder DEGs,
237including the “Axon guidance”, “Adherens junction” and “Focal adhesion” also
238exhibited over-represented in the GO terms targeted by the DMGs (S9 Fig).

239RNA-Seq data validation

240 To examine the reliability of the RNA-seq results, three DEGs (MyoD1, Six1
241and Ctnnb1) involved in the development of skeletal muscle were selected for
242validation using qRT-PCR. The mRNA expression levels of these key genes, such as
243Ctnnb1 related to cytoskeleton and cell adhesion, was down-regulated in the
244JP2_VS_JP1 comparison groups; Six1 corrected with regulation of skeletal muscle
245cell proliferation and skeletal muscle fiber development and MyoD1 in connection
246with positive regulation of myobalst differentiation and skeletal muscle cell
247differentiation, were all up-regulated in the JP2_VS_JP1 comparison groups,
248respectively. As shown in Fig 8, the qRT-PCR expression patterns of the three DEGs
249were in agreement with the RNA-seq data.

250Association analysis of methylRAD and the transcriptome (RNA-Seq).

251 The association analyses between the transcriptome and methylation were based
252on RNA-Seq and MethylRAD sequencing data. We calculated each gene's
253methylation level and expression level in larval, juvenile and adult female and adult
254male period Japanese flounder in terms of DNA methylation and the mRNA
255transcriptome. We observed that methylation levels correlates negatively with
256expression levels in both the CCGG and CCWGG pattern in larval, juvenile and adult
257Japanese flounder skeletal muscle tissue (Fig 9B). Furthermore, to explore the
258relationship between these DMGs and the DEGs found at the transcriptome level, an
259association analysis was performed. We found that a lot of genes that both different
260methylated and didfferent expressed in the JP2_VS_JP1, JP3_VS_JP1 and

261JP4_VS_JP1 comparison groups, respectively. However, only few genes
262simultaneously showed differential expression levels and DNA methylation levels in
263the JP2_VS_JP3, JP2_VS_JP4 and JP3_VS_JP4 comparison groups, respectively (Fig
2649A and S5 Table). We speculate that DNA methylation mainly affects skeletal muscle
265development in the larval period, and differences in skeletal muscle between juvenile
266and adult period Japanese flounder may be affected by other factors rather than DNA
267methylation, and that require further research.

268 Among these DEGs which also exhibited differential methylation levels, a large
269proportion of them appeared to be negatively correlated with their DNA methylation
270levels in the JP2_VS_JP1, JP3_VS_JP1 and JP4_VS_JP1 comparison groups,
271respectively. The results show a total of 238 and 187 negatively correlated genes with
272methylation in the JP1 and JP2 libraries, a total of 273 and 125 negatively correlated
273genes with methylation in the JP1 and JP3 libraries, a total of 310 and 119 negatively
274correlated genes with methylation in the JP1 and JP4 libraries in the CCGG and
275CCWGG site, respectively. These results suggest that DNA methylation makes a
276difference in the skeletal muscle during the developmental stages from larval to
277juvenile and adult Japanese flounder.

278 In the result, 118 were methylation down-regulated and expression up-regulated
279and 307 were methylation up-regulated and expression down-regulated in the skeletal
280muscle during the JP2_VS_JP1 comparison group. 118 were methylation down-
281regulated and expression up-regulated and 280 were methylation up-regulated and
282expression down-regulated in the skeletal muscle during the JP3_VS_JP1 comparison

283group. 132 were methylation down-regulated and expression up-regulated; and 307
284were methylation up-regulated and expression down-regulated in the skeletal muscle
285during the JP4_VS_JP1 comparison group (S5 Table).

286 To further investigate the signaling pathway associated with negatively
287correlated genes with methylation and expression levels in juvenile and adult compare
288to larval period, we performed KEGG enrichment analysis of these genes. The results
289showed that there were significantly enriched KEGG signaling pathway ($P < 0.05$)
290between larval and juvenile, between larval and female male adult, and between larval
291and male adult Japanese flounder, respectively (S10 Fig). In our study, KEGG
292enrichment analysis screens criteria for pathway entries with the number of
293differential genes greater than 2, however, there are too few differential genes to show
294in adult female and adult male compared to juvenile Japanese flounder and between
295adult female and adult male Japanese flounder, respectively. The pathway terms
296showing the highest level of significance were the Adherens junction, Axon guidance,
297Focal adhesion, cell junctions, actin cytoskeleton, Wnt signaling pathways and Hippo
298signaling pathway involved in the regulation of growth and development of skeletal
299muscle are shown.

300**Discussion**

301 **DNA methylation and mRNAs have been studied extensively in the**
302**past decades. However, a few studies have focused on Japanese flounder, one of**
303**the important economic Mariculture animals. This study is the first to compare**
304**systematically the genome-wide skeletal muscle DNA methylation profiles and**

305**their relationships to mRNA of larval, juvenile, adult female and adult male**
306**Japanese flounder. This study provided a comparative analysis of DNA**
307**methylation profiles of Japanese flounder muscle by MethyIRAD. Our data**
308**showed almost the entire genome with enough depth to identify differentially**
309**methylated regions with high accuracy and proved that MethyIRAD is a cost-**
310**effective approach for comprehensive analyses of the vertebrate genome-wide**
311**DNA methylation.**

312 Previous studies shows that DNA methylation is unevenly distributed in
313genomes, DNA methylation is enriched in the gene body regions, and depleted in the
314TSS and TTS [21-23]. And the intergenic regions is usually hypermethylated, while
315promoter regions of genes are relatively hypomethylated compared with the intragenic
316regions [8,22,24]. Japanese flounder displays analogous methylation pattern with that
317species. In our analysis, hypermethylation occurred not only at intergenic, gene body
318regions but also at introns, whereas the promoter (around TSSs) remains
319hypomethylated. The intracellular hypermethylation in the Japanese flounder genome
320further indicates that this methylation pattern may be a more conservative mechanism
321among species. In contrast to previous research in animals [8,25-26], we did not
322observe a higher methylation level in exons than in introns in Japanese flounder.

323 DNA methylation is one of the main epigenetic modification mechanisms, the
324analysis of DMRs within individuals is important. In several studies, different levels
325of DNA methylation could regulate stage-specific transcription and may be important
326during development and differentiation [27]. Thus, the analysis of DMRs among

327stages is essential in understanding stage-specific gene expression. We also observed
328that distribution of DNA methylation in the four groups showed generally conserved
329pattern, some DMRs were detected a high density in the intergenic, gene body and
330introns and a low density in the TSS200, TSS1500 and first exon regions. The first
331exon contained relatively few DMRs within the gene body, which may be the result of
332certain motifs overlapping between the promoter and the first exon. DNA
333methylation, especially intronic DNA methylation, may be associated with alternative
334splicing [28].

335 The DNA methylation status of promoter and gene body regions play an
336important role in the regulation of gene expression regulation via alteration in
337chromatin structure or transcription elongation efficiency [29-31]. Most of the
338promoter regions were hypomethylated in the vertebrate genome and one long
339established role of DNA methylation in gene promoter regions is the repression of
340gene expression [32,33]. Previous studies have demonstrated that DNA methylation in
341gene body regions impeded transcription elongation in Human, chicken, Neurospora
342crassa and Arabidopsis thaliana [22-23,34-35]. Methylation of these elements is
343known to be a crucial factor in the maintenance of genomic stability through the
344suppression of transcription, transposition, and recombination [8]. Thus, these results
345suggest that methylation has important effects on gene transcription in individual with
346different developmental stages. However, DNA methylation is only one of the
347regulators that influence gene expression. Since the interactions between transcription
348factors and methylated DNA could impact gene expression regulation and chromatin

349remodelling, changes in methylation may affect the expression of a gene [36]. Further
350studies are needed to explore the complicated epigenetic mechanism underlying
351growing. In summary, differences in DNA methylation patterns and the status of
352DMRs in the four groups of different developmental stages may play a crucial role in
353the process of development and the corresponding gene expression.

354 In this study, we constructed RNA-seq and DNA methylation libraries from
355skeletal muscle tissues of different developmental stages using transcriptome
356sequencing and the MethylRAD methods and discovered some genes simultaneously
357showed differential expression levels and DNA methylation levels. In our study, we
358have identified a large proportion of negatively correlated genes in skeletal muscle
359from larval, juvenile and adult Japanese flounder using deep sequencing technologies.
360The results showed that there were more methylation up-regulated and expression
361down-regulated genes increased in the skeletal muscle in the JP2_VS_JP1,
362JP3_VS_JP1 and JP4_VS_JP1 comparison groups, respectively. A GO enrichment
363analysis of these negatively corrected genes revealed that the variation in skeletal
364muscle development was related to biological processes, such as positive regulation of
365skeletal muscle tissue growth, skeletal muscle fiber development, Adherens junction,
366cell junctions and axon guidance. Meanwhile, in the present study, the functional
367annotation indicated that a large proportion of genes were involved in several
368important signaling pathways, including Wnt signaling pathways, cell adhesion , tight
369junctions, Adherens junction, hippopotamus signaling pathway, axon guidance, Focal
370adhesion and cytoskeleton. Axon guidance refers to the process by which growing

371neural axons follow specific, predictable paths to reach their target locations [37].
372Differential methylation changes in this pathway were used as a focus to identify how
373epigenetic changes during aging could potentially associate with the well-known
374decrease of skeletal muscle function with increasing age [38]. In addition, we also
375found the signaling networks that guide diverse cell behaviours and functions are
376connected to tight junctions transmitting information to and from the cytoskeleton
377[39], enriched. Previous research showed that the tight junction participated in the
378regulation of cell growth and differentiation, while adherens junctions participate in
379contact inhibition of cell growth [40,41]. Several studies, within the last decades,
380showed that Wnt signaling pathways are involved in myogenesis
381and regulate muscle formation. In myogenesis, the effect of Wnt signaling leads to the
382progression of the differentiation at early developmental stages and inhibition of this
383signaling leads to a poor skeletal muscle formation [42-44]. Remodeling of the actin
384cytoskeleton is critical for mediating changes in many fundamental processes
385including the cell shape, migration, and adhesion. The regulation of actin cytoskeleton
386is regulated by a large group of actin binding proteins that modulate actin assembly,
387disassembly, branching, and bundling, which form actin filament architecture and
388make it performing various specialized functions [45]. These results have provided
389direct evidence suggest that DNA methylation may be related to the skeletal muscle
390development in Japanese flounder. We believe that the differentially methylation of
391these genes might partially contribute to the Japanese flounder growth difference
392during different developmental period. However, the epigenetic effects of these genes

393on Japanese flounder growth still require further study in the future. This study
394expands the Japanese flounder methylated genes and could initiate further study in the
395muscle development of Japanese flounder.

396 In addition, We discovered some differentially DNA methylated genes involved
397in skeletal muscle development in larval, juvenile and adult Japanese flounder. For
398example, we found that MyoD1, a master regulatory gene of skeletal muscle
399differentiation [46]. Another well-known gene named myf6 (MRF4) is involved in
400inducing fibroblasts to differentiate into myoblasts and affects skeletal muscle
401development [47]. Six1 has been shown to play a pivotal role in skeletal muscle
402development [48-50] which is a transcription factor essential for embryonic
403myogenesis and also regulates MyoD1 expression in muscle progenitor cells. In
404addition, a recent study shows that Six1 contributes to the regeneration of adult
405muscle by enhancing and maintaining MyoD1 expression in adult muscle satellite
406cells in addition to its role in embryonic muscle formation [51]. MyoD1 is able to
407promote the transformation of multipotent stem cells to skeletal muscle by binding
408and activating the expression of a subset of pre-myogenic mesoderm genes,
409including Six1[52]. And gene Ctnnb1 modulates skeletal muscle development by
410acting on transcription factors controlling myogenesis such as MyoD[53].

411 We believed that the methylation of these genes might partially contribute to the
412Japanese flounder growth difference. However, the epigenomic regulation of
413molecular basis of skeletal muscle among different stages of Japanese flounder

414growth, which contributes to muscle growth-related genes, is still unclear and require
415further study in the future.

416**Conclusions**

417 We have generated the genome-wide profile of DNA methylation in Japanese
418flounder for the first time, and our results can be used for depth analyses of the roles
419played by DNA methylation in Japanese flounder and make that enriches research in
420molecular and developmental biology in vertebrates. Together, the work performed in
421this study probably aid in searching for epigenetic biomarkers for muscle growth
422regulation and promoting further development of Japanese flounder as a model
423organism for muscle research in other vertebrates.

424**Materials and methods**

425**Ethics statement**

426 All experimental procedures and sample collection were conducted according to the
427guidelines and were approved and supervised by the respective Animal Research and
428Ethics Committees of Ocean University of China. The field studies did not involve
429endangered or protected species. The fish were all euthanized by tricaine
430methanesulfonate (MS-222).

431**Experimental fish and data collection**

432 The experimental animals were collected from Donggang District Institute of
433marine treasures in Rizhao of Shandong province, and were temporary reared in a
434500L bucket in seawater in Ocean University of China within the same environment.

435 About 1000 individuals of larval 7dph (about 50 individuals as one sample) (stage
436 JP1), 40 individuals of juvenile about 90dph (stage JP2), and 80 individuals of adult
437 about 24 months (stage JP3 and JP4) were collected. During our experiment and data
438 analysis, the fish of stage JP1 were too small, so we used about 50 individuals as one
439 sample, other groups included three individuals, which were regarded as biological
440 replicates. All fish were sacrificed in compliance with the international guidelines for
441 experimental animals using tricaine methanesulfonate (MS-222). All fresh skeletal
442 muscle samples were collected (In stage A, we cut off redundant tissue and only retain
443 muscle tissue under the microscope) and the tissues were immediately frozen in liquid
444 nitrogen and then stored at -80°C until DNA and RNA extractions.

445 **DNA sample isolation and MethyRAD library construction and high-throughput** 446 **sequencing**

447 Genomic DNA of the four Japanese flounder groups was extracted from skeletal
448 muscle tissues with TIANamp Marine Animals DNA Kit (Cat No. DP324-
449 03) according to the manufacturer's protocol. The MethyRAD tag libraries were
450 constructed in 12 individuals with four groups following the protocol from Wang et
451 al. [16, 54]. The MethyRAD library was prepared by digesting 200 ng genomic DNA
452 for each sample using 4 U of the enzyme FspEI (NEB, USA) at 37°C for 4 h. Run 4
453 μl of digested DNA (~ 50 ng) on 1% agarose gel to verify the effectiveness of digestion.
454 FspEI can recognize 5-methylcytosine (5-mC) and 5-hydroxymethylcytosine (5-hmC)

455in the CmCGG and mCCWGG sites, and generate a double-stranded DNA break on
456the 3' side of the modified cytosine at a fixed distance (N12/N16). Accordingly,
457symmetrical DNA methylated sites were bidirectionally cleaved by FspEI to generate
45832-base-long fragments. Then, two adaptors were added to the digested DNAs by T4
459DNA ligase (NEB, USA), and the ligation products were amplified in 20 µl reactions
460by specific primers. PCR products were purified using a MinElute PCR Purification
461Kit (Qiagen) and pooled for sequencing using the Illumina X-ten PE 150 sequencing
462platform[16]. Base quality values were calculated using a Phred quality score (Q
463sanger = $-10\log_{10}p$). Input sequencing data before operation and computing were
464called raw reads. Raw reads were first subject to quality filtering and adaptor
465trimming. After operation, the data, including adapter reads and low-quality
466sequences, were removed from raw reads as clean reads.

467DNA methylation data analysis

468 To improve the accuracy in the following analysis, filtering pair-end sequencing
469paired clean reads according to the following terms: (i) remove low quality reads
470(more than 20% of base mass lower than 20), (ii) remove reads containing adapter and
471(iii) remove sequences containing too many N bases. The clean reads that did not
472contain the expected FspEI restriction site were further excluded, and the reads
473containing the methylated CCGG or CCWGG sites, named MethylRAD-tags, were
474identified. The MethylRAD-tags were subsequently aligned against the reference
475genome of Japanese flounder ([http://ftp.ncbi.nlm.nih.gov/genomes/all/GCF/001/970/005/
476GCF_001970005.1_Flounder_ref_guided_V1.0/](http://ftp.ncbi.nlm.nih.gov/genomes/all/GCF/001/970/005/GCF_001970005.1_Flounder_ref_guided_V1.0/)

477GCF_001970005.1_Flounder_ref_guided_V1.0_genomic.fna.gz) by SOAP program
478(version 2.21, parameters: -M4-v2-r0) [55] with two mismatches allowed. DNA
479methylation sites with a sequence depth of no less than 3 were judged to be reliable.

480 The distribution and density of methylated cytosine sites on chromosomes were
481calculated. Furthermore, the distributions of the methylated cytosine sites on different
482elements of the gene region were evaluated. For relative quantification of MethylRAD
483data, the DNA methylation levels of the genes were then evaluated by summing the
484methylation levels of sites that were localized in the gene regions and were
485determined using the normalized read depth (reads per million, RPM) for each site.
486($\text{RPM} = (\text{read coverage per site} / \text{high-quality reads per library}) \times 1,000,000$). The
487correlation between samples of methylation levels was assessed using Pearson's
488correlation coefficient. Upstream and downstream of 2kb sections of the gene body,
489TSS and TTS were selected and summarized the DNA methylation level of the
490distribution trend of sequencing reads. In our study, for CG context methylation,
491certain methylated C sites are defined as hypermethylation sites, at which the
492methylation level is over 75%; and some others are defined as sites of
493hypomethylation, at which the methylation level is less than 75%. For non-CG
494context methylation, hyper- and hypomethylation sites are defined as those at which
495the methylation levels are over or under 25%, respectively.

496 The change in methylation level was assessed based on the sequencing depth
497information of each site in the relative quantitative results of methylation, using R
498package edge R [56]. A p-value <0.05 and $\log_2\text{FC} >1$ were considered statistically

499significant. The function of the gene was described by a GO and KEGG function
500enrichment analysis of the gene where the differential methylation site was located.
501The number of genes included in each GO entry and KEGG pathway was counted and
502the significance of gene enrichment for each GO entry and KEGG pathway was
503calculated using the hypergeometric distribution test [57], GO entries with the number
504of corresponding genes greater than 2 in three categories were screened and the GO
505enrichment analysis results. Differences were considered significant at $P < 0.05$.

506RNA library construction and high-throughput sequencing

507 Total RNAs were extracted using TRIzol reagent (Invitrogen, CA, USA)
508according to the manufacturer's protocol from the same Japanese flounder as in
509MethyIRAD analysis. RNA purity and quantification were evaluated using a
510NanoDrop ND-2000 spectrophotometer (Thermo Scientific). RNA integrity was
511assessed using the Agilent 2100 Bioanalyzer (Agilent Technologies, Santa Clara, CA,
512USA). RNAs with high purity were used in library construction by TruSeq Stranded
513Total RNA with Ribo-Zero Gold (illumina, Cat.No. RS-122-2301) according to the
514manufacturer's instructions. These libraries were used for sequencing analysis with
515Illumina HiSeq X Ten platform and 150 bp paired-end reads were generated. To
516ensure the reliability of the sequencing data ,three fish were used to construct
517sequencing library during each developmental stage. In total, twelve RNA libraries
518were constructed and then sequenced with three technological replicates.

519Transcriptome data analysis and functional annotation

520 Clean reads were generated by filtering the low-quality reads, reads containing
521 adapter, reads containing ploy-N from the raw reads of fastq form by NGS QC Toolkit
522 [58]. All clean reads with high quality were annotated and classified by mapping them
523 to the Japanese flounder reference genome by Tophat (<http://tophat.cbcb.umd.edu/>).
524 The expressed genes were confirmed based on the annotation information of the clean
525 reads. The expression level of each gene was calculated and normalized by the
526 fragments per kilobase of transcript sequence per million base pairs sequenced
527 (FPKM) [59] using bowtie2 [60] and eXpress (v1.5.1) software [61].

528 Differential expression analysis of the genes was performed by using the DESeq
529 R package (2012). The NB (negative binomial distribution test) was used to test the
530 difference in the number of reads. The transcript expression was estimated by the
531 base mean value. The significantly DEGs between the two arbitrary samples were
532 identified based on the following thresholds: fold changes > 2 and P-values < 0.05 .
533 The assembled transcripts were annotated by Genomes (KEGG) and Gene Ontology
534 (GO). The relevant biological process, cellular component and molecular function of
535 the GO categories and KEGG biological pathways were identified through gene
536 enrichment analyses [62]. The hypergeometric test was conducted to identify the
537 significantly enriched GO terms and KEGG pathway (corrected p-value < 0.05).

538 **Quantitative RT-PCR**

539 The differential expression patterns of the genes detected by transcriptome data
540 were validated by qRT-PCR analysis. The specific primer pairs were designed for the
541 detection of corresponding genes (S6 Table). The 18S gene from Japanese flounder

542 was selected as internal control. TB Green™ Premix Ex Taq™ II (TliRNaseH Plus)
543 (Takara, Japan, Codeno. RR820A) in the StepOnePlus Real-Time PCR System was
544 used in the experiments. The relative expression levels of the genes were calculated
545 by the comparative $2^{-\Delta\Delta CT}$ method according to the manufacturer's
546 recommendations [63]. Three sample from each developmental stage were used, and
547 three technological replicates were performed to ensure the reliability of quantitative
548 analysis.

549 **MethylRAD data validation via BSP**

550 To validate the results obtained with MethylRAD data, three different methylated
551 genes among developmental stages related to skeletal muscle growth were selected
552 in the Japanese flounder genome for analysis by bisulfite sequencing. Three pairs of
553 bisulfite sequencing PCR (BSP) Primers were designed with Oligo 6.0
554 (<http://www.urogene.org/cgi-bin/methprimer/methprimer.cgi>) according to the known
555 sequences (S7 Table). Genomic DNA was extracted from muscle samples at different
556 developmental stages using Marine Animal DNA Kit (TransGen, Beijing, China)
557 following the manufacturer's instructions. The concentration and purity of DNA were
558 measured by the nucleic acid analyzer Biodropsis BD-1000 (OSTC, China), and the
559 integrity of DNA was evaluated by agarose gel electrophoresis. The Genomic DNA
560 was stored at -20°C for later use. In each developmental stage three fish were used to
561 process the bisulfite modification. Bisulfite modification of 200 ng of genomic DNA
562 was performed using the BisulFlash DNA Modification Kit (EpiGentek, USA) by
563 standard methods. The bisulfite-treated DNA was amplified by PCR with BSP

564specific primer pair. After a hot start, PCRs were carried out for 40 cycles of 94°C for
56540 sec, 50-55°C for 40 sec, and 72°C for 40 sec. PCR products were separated on a
5661.5% agarose gel, purified with the TIANGEN gel extraction kit and cloned into the
567pEASY-T1 vector (TransGen, Beijing, China) and transferred into Trans1-T1 Phage
568Resistant Chemically Competent Cell (TransGen, China). About ten typically positive
569clones were selected for each gene and subsequently sequenced to determine the
570methylation level.

571**Supporting information**

572**S1 Fig. Base distribution and quality distribution maps of clean reads.**

573**(PDF)**

574**S2 Fig. Comparison of DNA methylation patterns in the four groups.**

575**(PDF)**

576**S3 Fig. Hierarchical cluster analysis heat-map of differential methylation sites**

577**between groups.**

578**(PDF)**

579**S4 Fig. Methylation levels of DMRs in different groups.**

580**(PDF)**

581**S5 Fig. The distribution of DMR regions of different functional components.**

582**(PDF)**

583**S6 Fig. GO enrichment analysis of differential methylation site-related genes on**
584**top30 bar graph.**

585**(PDF)**

586**S7 Fig. KEGG enrichment analysis of differential methylation site-related genes**

587on top20 Signaling pathway.

588(PDF)

**589S8 Fig. Gene ontology classification of differentially expressed unigenes among
590groups.**

591(PDF)

592S9 Fig. KEGG enrichment top20 bubble chart among groups.

593(PDF)

**594S10 Fig. Annotations and The functional enrichment of genes with significantly
595negative correlated methylation and expression levels.**

596(PDF)

597S1 Table. Sample sequencing data volume and match rate.

598(PDF)

599S2 Table. DNA methylation site coverage depth in each sample.

600(PDF)

601S3 Table. The statistics of Reference genome comparison rate.

602(PDF)

603S4 Table. The analysis of differentially expressed genes among the four groups.

604(PDF)

605S5 Table. Statistics of differentially methylated and expressed genes.

606(PDF)

**607S6 Table. Nucleotide sequences of primers used for Real Time PCR in the
608experiment.**

609(PDF)

610S7 Table. Primers used for bisulphate PCR(BS-PCR).

611(PDF)

612Acknowledgments

613We thank editors and reviewers for comments on the manuscript.

614Author Contributions

615**Conceptualization:** Jingru Zhang, Feng He.

616**Funding acquisition:** Feng He.

617**Investigation:** Shuxian Wu, Yajuan Huang, Haishen Wen, Meizhao Zhang, Jifang

618Li, Yun Li, Xin Qi.

619**Writing – original draft:** Jingru Zhang.

620**Writing – review & editing:** Jingru Zhang, Feng He.

621References

6221. [Egger G](#), [Liang G](#), [Aparicio A](#), [Jones PA](#). Epigenetics in human disease and prospects for epigenetic

623therapy. [Nature](#). 2004;429(6990):457-63.

6242. [Thomas A. Down](#), [Vardhman K. Rakyan](#), [Daniel J. Turner](#), [Paul Flicek](#), [Heng Li](#), [Eugene Kulesha](#) et

625al. A Bayesian deconvolution strategy for immunoprecipitation-based DNA methylome analysis. [Nat](#)

626[Biotechnol](#). 2008 Jul; 26(7): 779–785.

6273. Sasaki H, Allen ND, Surani MA: DNA methylation and genomic imprinting in mammals. *EXS*.

6281993; 64:469–486.

6294. Courtier B, Heard E, Avner P: Xce haplotypes show modified methylation in a region of the active

630X chromosome lying 3' to Xist. *Proc Natl Acad Sci U S A* 1995,92(8):3531–3535.

6315. Siegfried Z, Eden S, Mendelsohn M, Feng X, Tsuberi BZ, Cedar H: DNA methylation represses
632transcription in vivo. *Nat Genet.* 1999;22(2):203–206.
6336. Bird A: DNA methylation patterns and epigenetic memory. *Genes Dev.* 2002; 16(1):6–21.
6347. Eckhardt F, Lewin J, Cortese R, Rakyan VK, Attwood J, Burger M, et al. DNA methylation
635profiling of human chromosomes 6, 20 and 22. *Nat Genet.* 2006;38:1378–1385.
6368. [Sati S](#), [Tanwar VS](#), [Kumar KA](#), [Patowary A](#), [Jain V](#), [Ghosh S](#), et al. High resolution methylome map
637of rat indicates role of intragenic DNA methylation in identification of coding region. [PLoS](#)
638[One](#). 2012;7(2):e31621.
6399. Sandra Cortijo René, Wardenaar, Maria Colomé-Tatché, Frank Johannes, Vincent Colot.
640Sandra Cortijo, et al. Genome-Wide Analysis of DNA Methylation in Arabidopsis Using MeDIP-Chip.
641[Plant Epigenetics and Epigenomics](#). 2014;1112:125-149.
64210. Buckingham M, Vincent SD. Distinct and dynamic myogenic populations in the vertebrate
643embryo. *Curr Opin Genet Dev.* 2009;19(5):444–53.
64411. Buckingham M. Skeletal muscle formation in vertebrates. *Curr Opin Genet Dev.* 2001;11:440–8.
64512. Larsen F, Gundersen G, Lopez R, Prydz H: CpG Islands as gene markers in the human genome.
646*Genomics.* 1992; 13(4):1095–1107.
64713. Plass C, Soloway PD: DNA methylation, imprinting and cancer. *Eur J Hum Genet.* 2002; 10(1):6–
64816.
64914. Su ZX, Xia JF, Zhao ZM. Functional complementation between transcriptional methylation
650regulation and post-transcriptional microRNA regulation in the human genome. [BMC Genomics](#). 2011;
65112(Suppl 5):S15.
65215. Frommer M, McDonald LE, Millar DS, Collis CM, Watt F, et al. A genomic sequencing protocol
653that yields a positive display of 5-methylcytosine residues in individual DNA strands. *Proc Natl Acad*

654Sci U S A . 1992; 89:1827–1831.

65516. Wang S, Lv J, Zhang L, Dou J. MethylRAD: a simple and scalable method for genome-wide DNA

656methylation profiling using methylation dependent restriction enzymes. *Open Biol.* 2015;150130:5.

65717. [Cohen-Karni D](#), [Xu D](#), [Apone L](#), [Fomenkov A](#), [Sun Z](#), [Davis PJ](#), et al. The MspJI family of

658modification-dependent restriction endonucleases for epigenetic studies. *Proc Natl Acad Sci U S A.*

6592011;108,11040–11045.

66018. [Zhang Y](#), [Liu J](#), [Fu W](#), [Xu W](#), [Zhang H](#), [Chen S](#), et al. Comparative Transcriptome and DNA

661methylation analyses of the molecular mechanisms underlying skin color variations in Crucian carp

662(*Carassius carassius* L.). *BMC Genet.* 2017;18(1):95

66319. [Li H](#), [Yuan J](#), [Wu M](#), [Han Z](#), [Li L](#), [Jiang H](#), et al. Transcriptome and DNA methylome reveal

664insights into yield heterosis in the curds of broccoli (*Brassica oleracea* L var. *italica*) *BMC Plant*

665*Biol.* 2018;18(1):168.

66620. Krueger F, Andrews SR. Bismark: a flexible aligner and methylation caller for bisulfite-Seq

667applications. *Bioinformatics.* 2011;27(11):1571–2.

66821. Weber M, Davies JJ, Wittig D, Oakeley EJ, Haase M, Lam WL, Schuebeler D: Chromosome-wide

669and promoter-specific analyses identify sites of differential DNA methylation in normal and

670transformed human cells. *Nat Genet.* 2005;37(8):853–862.

67122. Li Q, Li N, Hu X, Li J, Du Z, Chen L, Yin G, Duan J, Zhang H, Zhao Y: Genome-wide mapping of

672DNA methylation in chicken. *Plos One.* 2011;6(5):e19428.

67323. Zhang X, Yazaki J, Sundaresan A, Cokus S, Chan SW-L, Chen H, Henderson IR, Shinn P,

674Pellegrini M, Jacobsen SE: Genome-wide high-resolution mapping and functional analysis of DNA

675methylation in arabidopsis. *Cell.* 2006;126(6):1189–1201.

67624. Ball MP, Li JB, Gao Y, Lee JH, LeProust EM, Park I-H, et al. Targeted and genome-scale strategies

- 677 reveal gene-body methylation signatures in human cells. *Nat Biotechnol.* 2009, 27(4):361–368.
67825. [Laurent L](#), [Wong E](#), [Li G](#), [Huynh T](#), [Tsirigos A](#), [Ong CT](#), et al. Dynamic changes in the human
- 679 methylome during differentiation. [Genome Res.](#) 2010;20(3):320-31.
68026. [Feng S](#), [Cokus SJ](#), [Zhang X](#), [Chen PY](#), [Bostick M](#), [Goll MG](#), et al. Conservation and divergence of
- 681 methylation patterning in plants and animals. [Proc Natl Acad Sci U S A.](#) 2010;107(19):8689-94.
68227. Long J, Jing Z, Xia YD, Lou P, Chen L, Wang HM, et al. Genome-wide DNA methylation changes
- 683 in skeletal muscle between young and middle-aged pigs. [BMC Genomics.](#) 2014;15(1):653.
68428. Shukla S, Kavak E, Gregory M, Imashimizu M, Shutinoski B, Kashlev M, et al. CTCF-promoted
- 685 RNA polymerase II pausing links DNA methylation to splicing. *Nature.* 2011;479(7371):74–79.
68629. Lorincz MC, Dickerson DR, Schmitt M, Groudine M. Intragenic DNA methylation alters
- 687 chromatin structure and elongation efficiency in mammalian cells. *Nat. Struct. Mol. Biol.* 2004;11,
- 688 1068–1075.
68930. Klose RJ, Bird AP. Genomic DNA methylation: the mark and its mediators. *Trends Biochem. Sci.*
- 690 2006;31,89–97.
69131. Suzuki MM, Bird A. DNA methylation landscapes: provocative insights from epigenomics. [Nat](#)
- 692 [Rev Genet.](#) 2008;9(6):465-76.
69332. Li MZ, Wu HL, Luo ZG, Xia YD, Guan JQ, Wang T, et al: An atlas of DNA methylomes in
- 694 porcine adipose and muscle tissues. *Nature communications.* 2012;3:850.
69533. Klose RJ, Bird AP: Genomic DNA methylation: the mark and its mediators. *Trends Biochem Sci.*
- 696 2006;31(2):89–97
69734. Lorincz MC, Dickerson DR, Schmitt M, Groudine M. Intragenic DNA methylation alters
- 698 chromatin structure and elongation efficiency in mammalian cells. [Nat Struct Mol](#)
- 699 [Biol.](#) 2004;11(11):1068-75.

70035. Rountree MR, Selker EU. DNA methylation inhibits elongation but not initiation of transcription
701in *Neurospora crassa*. [Genes Dev.](#) 1997;11(18):2383-95.
70236. [Zhu H](#), [Wang G](#), [Qian J](#). Transcription factors as readers and effectors of DNA methylation [Nat Rev](#)
703[Genet.](#) 2016;17(9):551-65.
70437. Harel NY, Strittmatter SM. Can regenerating axons recapitulate developmental guidance during
705recovery from spinal cord injury? [Nat Rev Neurosci.](#) 2006;7(8):603-16.
70638. [Zykovich A](#), [Hubbard A](#), [Flynn JM](#), [Tarnopolsky M](#), [Fraga MF](#), [Kerksick C](#), et al. Genome-wide
707DNA methylation changes with age in disease free human skeletal muscle. [Aging](#)
708[Cell.](#) 2014;13(2):360-6.
70939. [Zihni C](#), [Mills C](#), [Matter K](#), [Balda MS](#). Tight junctions: from simple barriers to multifunctional
710molecular gates. [Nat Rev Mol Cell Biol.](#) 2016;17(9):564-80.
71140. Potter E, Bergwitz C, Brabant G. The cadherin-catenin system: implications for growth and
712differentiation of endocrine tissues. [Endocr Rev.](#) 1999;20(2):207-39.
71341. Bazzoni G, Dejana E. Endothelial cell-to-cell junctions: molecular organization and role in
714vascular homeostasis. [Physiol Rev.](#) 2004;84(3):869-901.
71542. [Tran TH](#), [Shi X](#), [Zaia J](#), [Ai X](#). Heparan Sulfate 6-O-endosulfatases (Sulfs) Coordinate the Wnt
716Signaling Pathways to Regulate Myoblast Fusion during Skeletal Muscle Regeneration. [J Biol Chem.](#)
7172012;287(39):32651–32664.
71843. [Cisternas P](#), [Henriquez JP](#), [Brandan E](#), [Inestrosa NC](#). Wnt Signaling in Skeletal Muscle Dynamics:
719Myogenesis, Neuromuscular Synapse and Fibrosis. [Mol Neurobiol.](#) 2014;49(1):574-89.
72044. van Amerongen R, Berns A. Knockout mouse models to study Wnt signal transduction. Trends
721Genet. 2006; 22(12):678–689.
72245. Roffers-Agarwal, J, Xanthos, JB, Miller JR. Regulation of actin cytoskeleton architecture by Eps8

723and Abi I. [BMC Cell Biol.](#) 2005;6:36.

72446. Tapscott SJ. The circuitry of a master switch: MyoD and the regulation of skeletal muscle gene

725transcription. *Development*, 2005,132(12):2685-2695.

72647. [Montarras D1](#), [Chelly J](#), [Bober E](#), [Arnold H](#), [Ott MO](#), [Gros F](#), et al. Developmental patterns in the

727expression of Myf5, MyoD, myogenin, and MRF4 during myogenesis. [New Biol.](#) 1991;3(6):592-600.

72848. Laclef C, Hamard G, Demignon J, Souil E, Houbron C, Maire P. Altered myogenesis in Six1-

729deficient mice. *Development*. 2003;130(10):2239–52.

73049. Grifone R, Demignon J, Houbron C, Souil E, Niro C, Seller MJ, et al. Six1 and Six4

731homeoproteins are required for Pax3 and Mrf expression during myogenesis in the mouse

732embryo. *Development*. 2005;132(9):2235–49.

73350. Richard AF, Demignon J, Sakakibara I, [Pujol J](#), [Favier M](#), [Strochlic L](#), et al. Genesis of muscle

734fiber-type diversity during mouse embryogenesis relies on Six1 and Six4 gene expression. *Dev*

735*Biol.* 2011;359(2):303–20.

73651. Liu Y, Chakroun I, Yang D, [Horner E](#), [Liang J](#), [Aziz A](#), et al. Six1 Regulates MyoD Expression in

737Adult Muscle Progenitor Cells. *PLoS One*. 2013;8(6):e67762.

73852. Gianakopoulos PJ, Mehta V, Voronova A, Cao Y, Yao Z, Coutu J, et al. MyoD directly up-regulates

739premyogenic mesoderm factors during induction of skeletal myogenesis in stem cells. *J Biol*

740*Chem.* 2011;286(4):2517–25.

74153. [Karczewska-Kupczewska M](#), [Stefanowicz M](#), [Matulewicz N](#), [Nikołajuk A](#), [Strączkowski M](#). Wnt

742Signaling Genes in Adipose Tissue and Skeletal Muscle of Humans With Different Degrees of Insulin

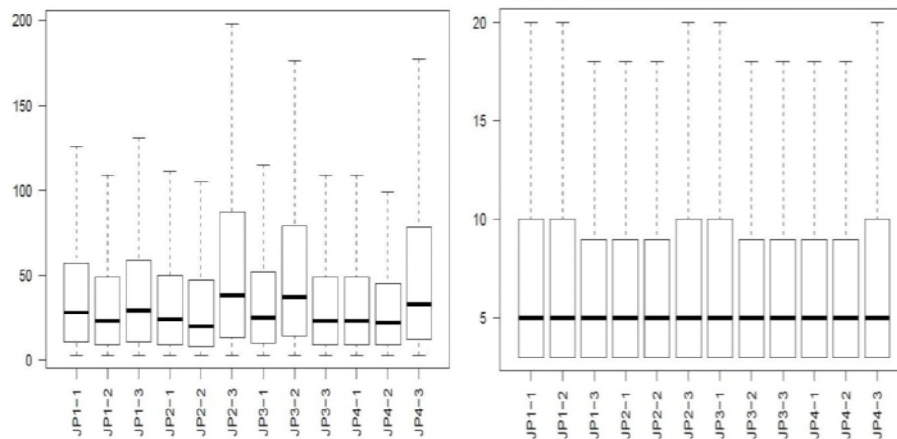
743Sensitivity. [J Clin Endocrinol Metab.](#) 2016 Aug;101(8):3079-87. doi: 10.1210/jc.2016-1594.

74454. [Wang S](#), [Liu P](#), [Lv J](#), [Li Y](#), [Cheng T](#), [Zhang L](#), et al. Serial sequencing of isologous RAD tags for
745cost-efficient genome-wide profiling of genetic and epigenetic variations. *Nature Protocols*, 2016,
74611(11):2189-2200.
74755. [Li R](#), [Yu C](#), [Li Y](#), [Lam TW](#), [Yiu SM](#), [Kristiansen K](#). SOAP2: an improved ultrafast tool for short
748read alignment. *Bioinformatics*. 2009;25(15):1966-7.
74956. [Robinson MD](#), [McCarthy DJ](#), [Smyth GK](#). edgeR: a Bioconductor package for differential
750expression analysis of digital gene expression data. *Bioinformatics*. 2010;26(1):139-40.
75157. [Cohen-Karni D](#), [Xu D](#), [Apone L](#), [Fomenkov A](#), [Sun Z](#), [Davis PJ](#), et al. The MspII family of
752modification-dependent restriction endonucleases for epigenetic studies. *Proc Natl Acad Sci U S*
753*A*. 2011;108(27):11040-5.
75458. Patel RK, Jain M. NGS QC Toolkit: A toolkit for quality control of next generation sequencing
755data. *PLoS ONE*. 2012; 7(2): e30619.
75659. [Trapnell C](#), [Williams BA](#), [Pertea G](#), [Mortazavi A](#), [Kwan G](#), [van Baren MJ](#), et al. Transcript
757assembly and quantification by RNA-Seq reveals unannotated transcripts and isoform switching during
758cell differentiation. *Nat Biotechnol*. 2010;28(5):511-5.
75960. Langmead B, Salzberg SL. Fast gapped-read alignment with Bowtie 2. *Nat*
760*Methods*. 2012;9(4):357-9.
76161. [Mortazavi A](#), [Williams BA](#), [McCue K](#), [Schaeffer L](#), [Wold B](#). Mapping and quantifying mammalian
762transcriptomes by RNA-Seq. *Nat Methods*. 2008;5(7):621-8.
76362. [Kanehisa M](#), [Araki M](#), [Goto S](#), [Hattori M](#), [Hirakawa M](#), [Itoh M](#), et al. KEGG for linking genomes
764to life and the environment. *Nucleic Acids research*. 2008;36:480-4.
76563. Livak KJ, Schmittgen TD: Analysis of relative gene expression data using real-time quantitative
766PCR and the 2(-Delta Delta C(T)) Method. *Methods*. 2001;25(4):402-8.

767

768**Fig 1. Sequencing depth box diagram of methylation site (CCGG and CCWGG) in each sample.**

769In the box diagram, the box part is the main body of the box-shaped chart, and the middle of the black
770horizontal line is the median of the data; the upper and lower sides of the box is a quarter of the data
771that are greater than the upper quartile (Q3), and a quarter of the data are less than the lower quartile
772(Q1). The interval between Q1 and Q3 is called the inter-quartile range (IQR). The longitudinal lines in
773the upper and lower sides of the box are tentacle lines. The upper cut off line of the tentacle line is
774“ $Q3+1.5 * IQR$ ” and the lower one is “ $Q1-1.5 * IQR$ ”.



775

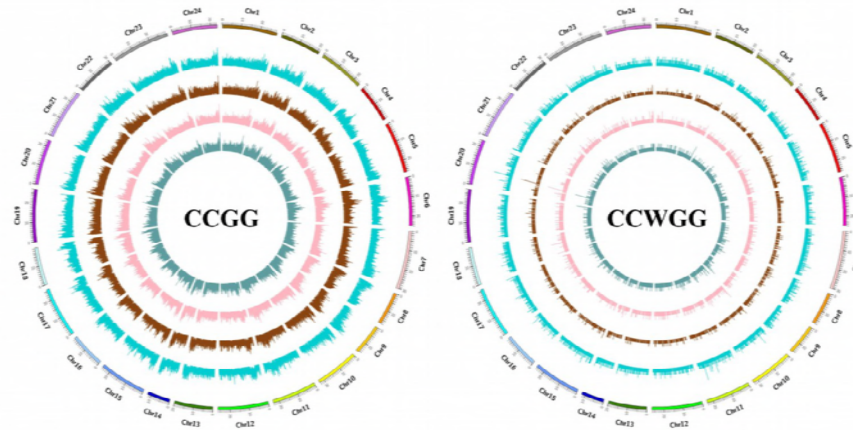
776

777**Figure 2. The distribution of DNA methylation sites in the CCGG and CCWGG on**

778**chromosomes.** The distribution of DNA methylation sites on chromosomes 1 to 24 of the Japanese

779flounder genome is shown for each sample. From the outside to the inside is JP1、JP2、JP3、JP4

780respectively.



781

782

783 **Figure 3. (A) DNA methylation site on different gene function components distribution**

784 **histogram.** 1stexon: the regions of the first exon; Body: the whole exons of genes(except 1stexon);

785 TSS200: the upstream 200 bp of the transcription termination site (TSS); TSS1500: the upstream 1500

786 bp of TSS; intron:the whole introns of genes ;“intergenic” indicated the intergenic regions (CCGG

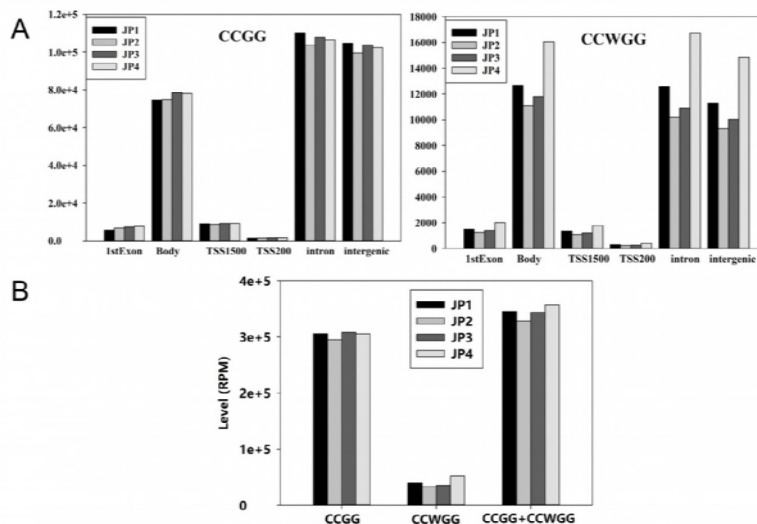
787 methylation sites is shown, left and CCWGG methylation sites is shown, right). The y-axis shows the

788 number of methylation sites. The x-axis shows the different components of the genome. **(B) DNA**

789 **methylation distributions of CCGG and CCWGG sites with differential methylation levels.** The

790 y-axis shows the number of methylation sites. The x-axis shows the CCGG, CCWGG sites and the

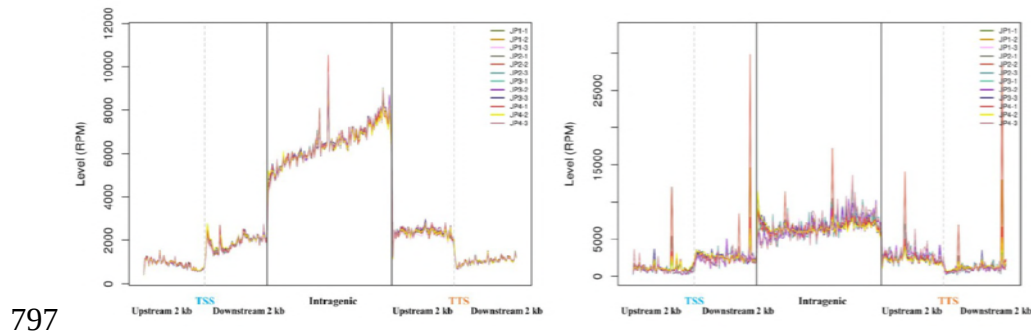
791 whole CCGG, CCWGG sites.



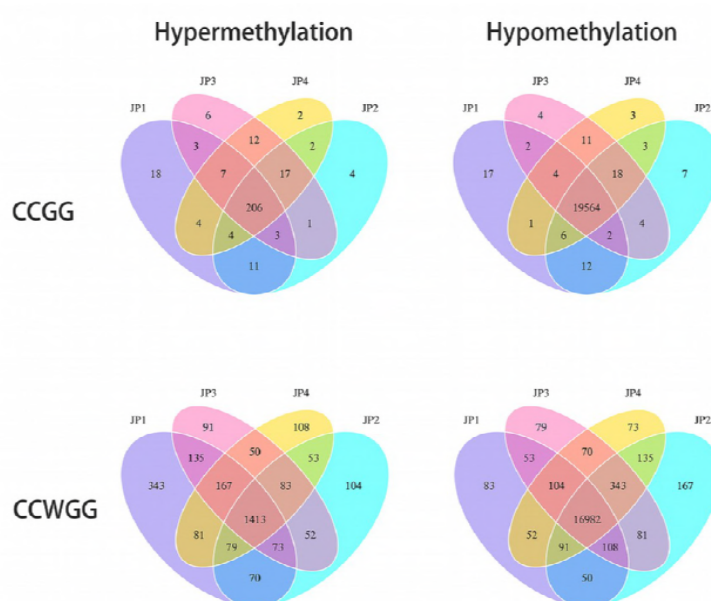
792

793 **Fig 4. Distribution of Methyl-RAD reads around gene bodies.** The x axis indicates the position

794 around gene bodies, and the y axis indicates the normalized read number. This figure reflects the
 795 methylation level around gene bodies. CCGG sites methylation level is shown, left and CCWGG sites
 796 methylation level is shown, right.

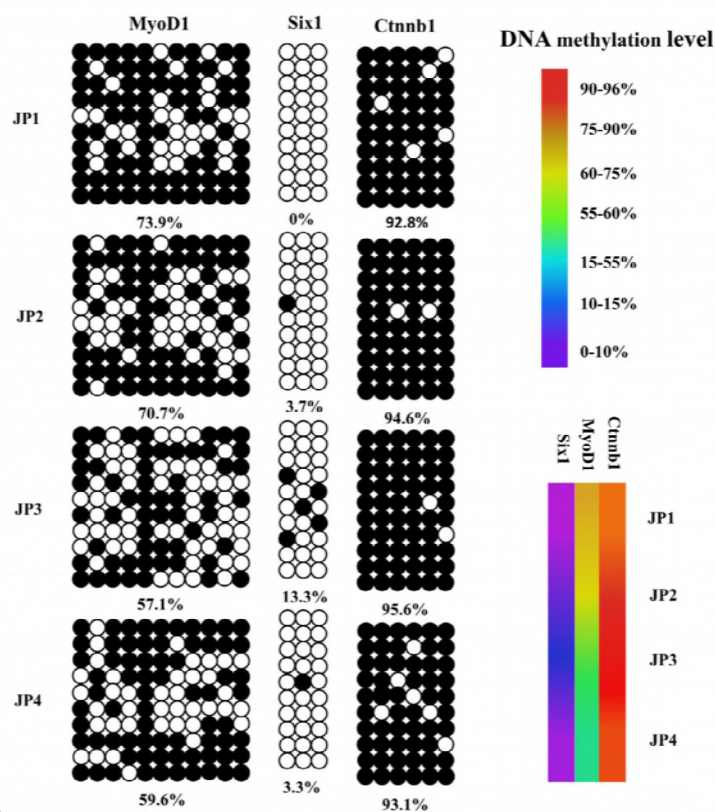


798 **Fig 5. The Venn diagram for comparison of DMRs that are unique or shared in four groups**
 799 **derived from Japanese flounder.** For CG context methylation, certain methylated C sites are defined
 800 as hypermethylation sites, at which the methylation level is over 75%; and some others are defined as
 801 sites of hypomethylation, at which the methylation level is less than 75%. For non-CG context
 802 methylation, hyper- and hypomethylation sites are defined as those at which the methylation levels are
 803 over or under 25%, respectively.



804
 805 **Fig 6. The validation of MethyRAD data by bisulfite sequencing (BSP).** Three genes obtained from

806MethylRAD data was selected randomly and its methylation pattern was profiled by BSP. The box
807indicated amplification regions. CpG dinucleotides are represented by circles on vertical bars. Each line
808represents an independent clone, and methylated CpGs are marked by filled circles, unmethylated
809CpGs by open circles. Average methylation was calculated for all CpG sites in each stage. There were
810three samples in each group, respectively and for each sample typically 10 clones were used to show
811DNA methylation levels. Different colors in the right show different methylation level.



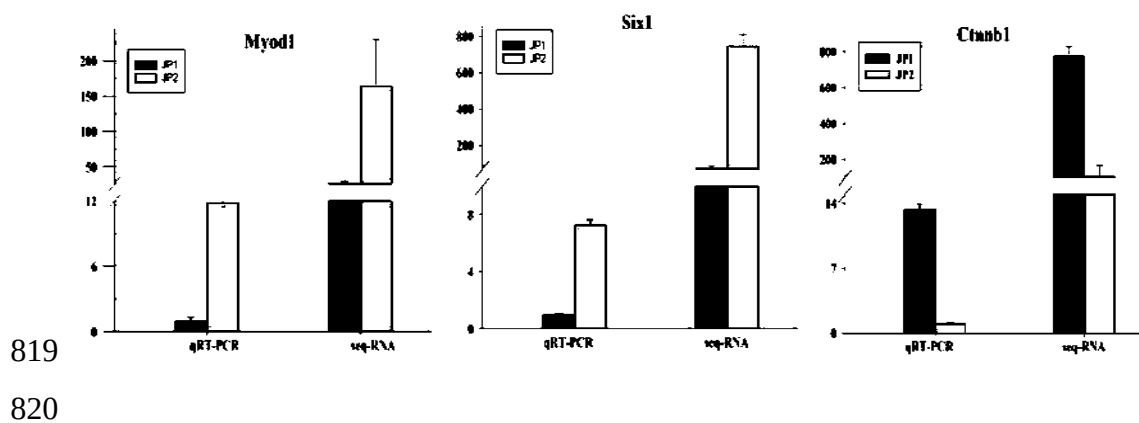
812

813Fig 7. The Venn diagram for comparison of DEGs that are unique or shared in four groups. DEG:

814Differently methylated genes

815

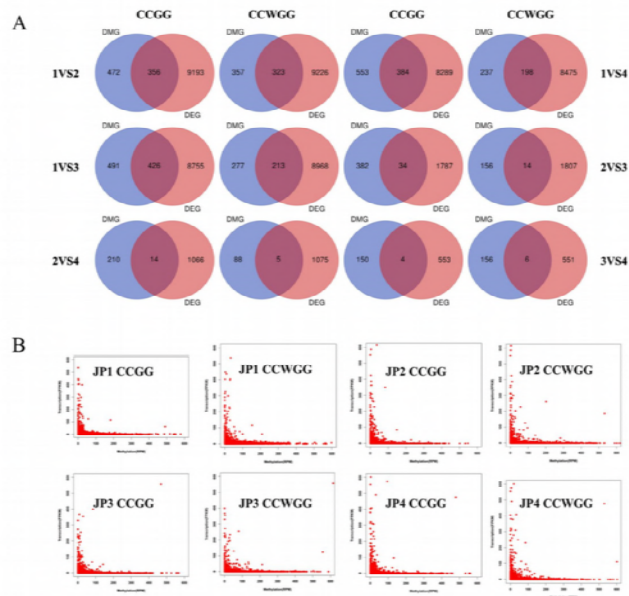
816**Fig 8. The validation of RNA-seq data by qRT-PCR.** Three genes obtained from RNA-seq data was
817selected and was validated by qRT-PCR. X axis indicated the relative RNA-seq and qRT-PCR results of
818genes. Y axis indicated the relative expression levels of genes.



819

820

821**Fig 9. Relationship of differential expression levels of genes and their DNA methylation levels.** a
822indicated the Venn diagrams of genes showing differential expression levels and/or differential DNA
823methylation levels by pairwise comparison analysis. DMG, differentially methylated gene; DEG,
824differentially expressed gene. b indicated the distribution characteristics of gene methylation and
825expression levels. JP1 (larval Japanese flounder); JP2 (juvenile Japanese flounder); JP3 (adult female
826Japanese flounder); JP4 (adult male Japanese flounder). X axis indicated the relative DNA methylation
827levels of genes. Y axis indicated the relative expression levels of genes.



828